NASA CONTRACTOR REPORT

RESEARCH AND DEVELOPMENT OF A SONIC BOOM SIMULATION DEVICE

by Roger Tomboulian

Prepared by
GENERAL APPLIED SCIENCE LABORATORIES, INC.
Westbury, N. Y.
for Langley Research Center

NATIONAL AERONAUTICS AND SPACE ADMINISTRATION • WASHINGTON, D. C. • JULY 1969

RESEARCH AND DEVELOPMENT OF A SONIC BOOM SIMULATION DEVICE

By Roger Tomboulian

Issued by Originator as Report No. GASL TR-713

Prepared under Contract No. NAS 1-7985 by
GENERAL APPLIED SCIENCE LABORATORIES, INC.
A Subsidiary of The Marquardt Corporation
Westbury, N.Y.

for Langley Research Center

NATIONAL AERONAUTICS AND SPACE ADMINISTRATION

For sale by the Clearinghouse for Federal Scientific and Technical Information
Springfield, Virginia 22151 – CFSTI price $3.00

FOREWORD

It is my pleasure to acknowledge the efforts of Dr. Manlio Abele for supplying some of the analysis, and to Messrs. William Peschke, Hans Giest, and Charles Sabin, for the construction and testing of the facility.

TABLE OF CONTENTS

LIST OF FIGURES

RESEARCH AND DEVELOPMENT OF A SONIC BOOM SIMULATION DEVICE

By Roger Tomboulian

General Applied Science Laboratories, Inc.
A Subsidiary of The Marquardt Corporation

INTRODUCTION

Growing concern has been voiced about the various effects due to the sonic boom generated by supersonic aircraft. Much of the character of the boom response is presently unclear, especially in regard to the influence on the boom of terrain, buildings and building materials, and atmospheric interaction. The need for a laboratory type simulator to generate sonic booms has been recognized.

Ideally, such a simulator should be capable of reproducing boom signatures of varying shapes, with variable pressure amplitudes and durations and be capable of changing these parameters in a simple and predictable manner. In addition, a proper simulation would also provide that the pressure wave be a traveling wave with the correct velocity corresponding to that produced by supersonic transport. Because many problems involving structural materials require numerous tests in order to obtain a statistically valid conclusion, the operation of the simulator should be economical on a per shot basis. Further, it would be highly desirable that the laboratory device be able to reduce the signature wavelength so that many tests can be performed using scale models which would allow obvious cost savings and extend the research potential.

To fulfill these requirements for a sonic boom simulator, a pilot facility using an air supply, a mass control valve, and a horn (or duct) was successfully constructed and operated. The purpose of the present study was to further develop this method of sonic boom simulation and to advance the understanding of the technology involved. The intent was to extend the technique to a larger, more useful facility size. Also included were improvements in valve design, duct wall structure, and duct terminal absorber.

To consider some of the problems associated with the sonic boom facility, an initial study was made of the various parameters governing operations to simulate sonic booms. From this study a design was initiated for a large fast-acting plug valve to control the mass flow. A conical duct made of reinforced concrete, a control building, and the hydraulic and pneumatic systems required to operate the device were designed and constructed. After an extensive program of analysis of the end reflection conditions, a unique solution was developed which permitted the cancellation of the outgoing wave without the need of a large classical absorber. The concept of this end termination is based on the fact that to match the complex acoustical admittance present at the end of the duct, both the resistive and inertial components of the pressure wave must be cancelled.

From this theoretical analysis an engineering program was conducted so that the required material and fabrication techniques could be identified. After an extensive search to locate the correct resistive type of material, a suitable compromise material was selected and the special moving absorber was fabricated. The initial results obtained using this impedance matching device on the end of the duct, while not perfect, indicate that the approach is conceptually sound and that a simulator device of reasonable length can be made and yet produce full-scale sonic boom signatures. The following sections of this report will detail the work outlined above, and will discuss the initial results obtained from this new facility. The report also indicates the technique that could be used in performing various research tasks with the facility.

LIST OF SYMBOLS

a	speed of sound
k	elastic spring constant (per unit area)
M	Mach number
p	absolute pressure (see subscript note)
$p-p_o=\bar{p}$	pressure of "boom" wave
r	radial coordinate
R	frictional resistance (per unit area)
R_1	viscous resistance (per unit area)
S	surface
t	time
u_r	velocity (radial)
V	piston velocity
w	mass flow rate
γ	specific heat, ratio
ω	angular frequency
Ω	cone solid angle
ρ	density
σ	absorber mass (per unit area)
τ	time coordinate associated with wave
τ_o	period of wave

Subscripts

o	ambient atmospheric conditions
∞	plenum or reservoir conditions
e	relates to an arbitrary reference station near the end of the duct
i	relates to shock interface
1	relates to condition upstream of the shock interface
r	reflected wave

GASL-NASA SIMULATOR FACILITY

As a first step in the design of a new and larger facility a comprehensive analysis of the physical parameters was undertaken. Although the results obtained from the pilot facility indicated that the general operation of the simulator was conceptually correct, the analysis is useful in pointing out the various limitations and potential trouble areas that may be encountered when the design is extrapolated. Hence, in Appendix A is described a semi-rigorous examination of the phenomena associated with this simulator which leads to a more complete understanding of its fundamental operation.

Based on this analysis a sonic boom simulator was built at GASL. A schematic of the final configuration is shown in Figure 1. Of interest here are the three main components of the simulator, namely the mass control valve, the conical duct and the cone termination (absorber). A photograph of some aspects of the simulator is presented in Figure 2.

Conical Duct

The basic construction of the conical duct was made to be extremely rigid so that there would be no loss of wave energy to the walls. Consequently, using standard design with an additional factor, the resulting wall thicknesses showed that 8" of 3000 lb reinforced concrete could provide the required degree of rigidity. Although the strength requirements of the walls diminish towards the small end of the cone, for ease of construction the entire pyramid was made with uniform walls. The 100 ft. long duct was made in three pieces with sealed expansion joints between them. The half cone angle was taken to be about $2\frac{1}{2}^{o}$ as a conservative figure so that no problems involving separation of the flow would exist.

Every effort was made to maintain the precision of the duct. Measurements indicate that the divergence from linearity is on the order of 1/4" at the center of the span. It is likely that such a small perturbation would not influence the basic operation of the simulator.

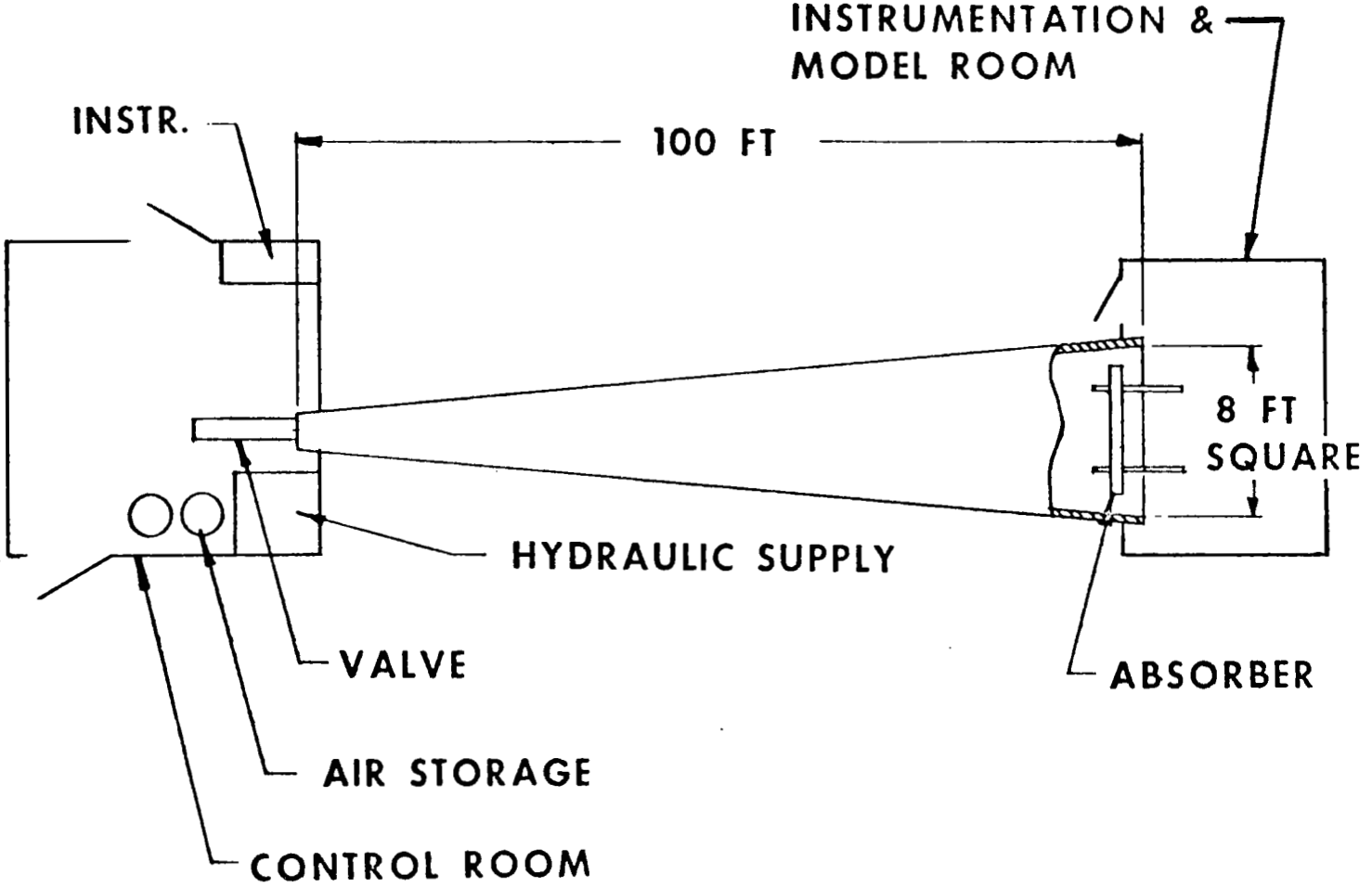

FIGURE 1

TEST FACILITY LAYOUT SCHEMATIC

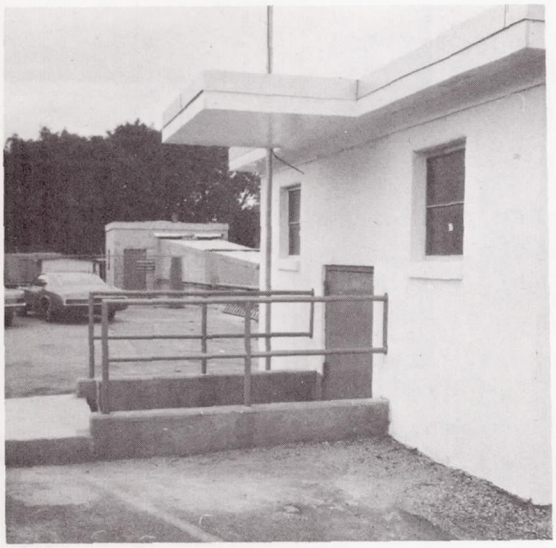

External Layout

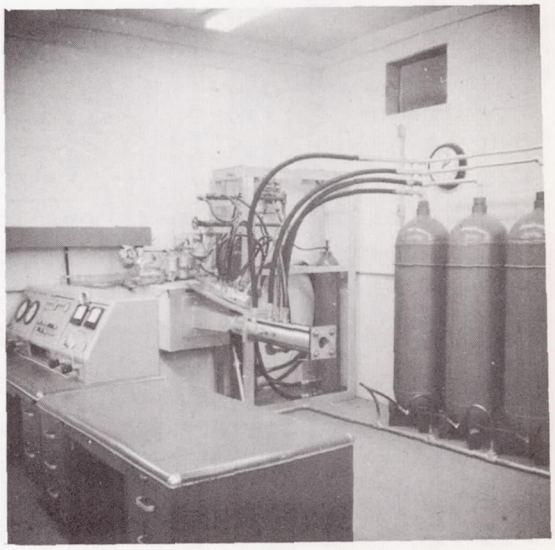

Internal View of
Control Room

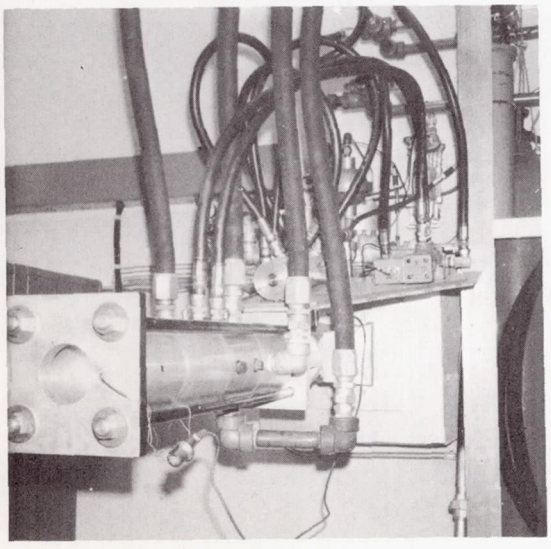

Plug valve with
operating lines

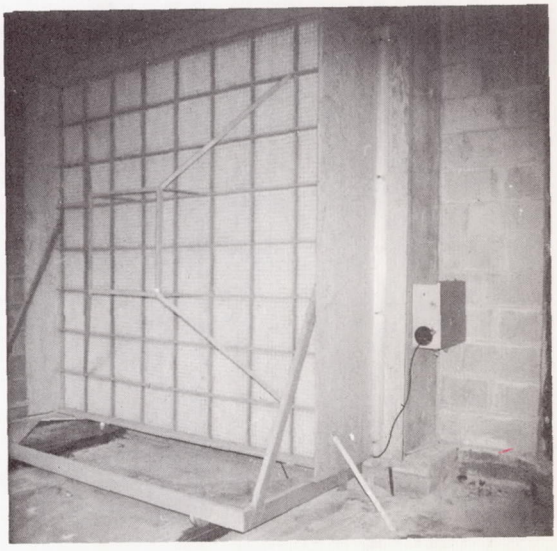

External view of
moving absorber

FIGURE 2 - SOME ASPECTS OF THE FACILITY

Valve

Fundamental to the analysis in Appendix A is the concept that the gas mass flow will be controlled (by a valve) as a function of time at the sonic orifice located at the origin of the conical duct.

The basic requirement of the valve mechanism is that it be able to prescribe a mass flow function of time at a position r_c downstream of the throat area. If the valve and transition to the conical duct are designed such that the valve is the limiting orifice in this flow system, then the mass flow through the valve will be just proportional to the opening area of such a throat. Hence by maintaining a high constant pressure in the reservoir, a condition of Mach 1 is always obtained at the throat region.

Let r* be the radial position of the throat from the virtual cone origin as shown in Figure 3. The cone region between r* and r_c may be considered as the transition region between the flow condition in the throat and the acoustic region of the cone. Thus for $r > r_c$ the acoustic approximation underlying the preceding analysis is valid. As previously indicated, all geometrical dimensions in the cone region between r* and r_c are small compared to the minimum wavelength of interest. Thus the fluid dynamic analysis in the throat region can be conducted to a first approximation as a sequence of steady state flow field calculations throughout the wave period except for the short time interval close to $\tau = 0$ and $\tau = \tau_o$. Such an approximation will more easily allow a physical understanding of the real system.

At any given instant of time during the wave period, the flow is supersonic downstream of the throat. A shock interface will be found at a given distance r_i as indicated in Figure 3 where the flow becomes subsonic. The position of the shock interface as shown is only representative of a possible location since such an interface moves in the duct as a function of the mass flow. On the basis of steady state isentropic one-dimensional fluid dynamic consideration the supersonic flow region is described by the equations

$$w = \rho_i \, u_{ri} \, S = \rho_1 \, u_{r1} \, r^2 \, \Omega \qquad (1)$$

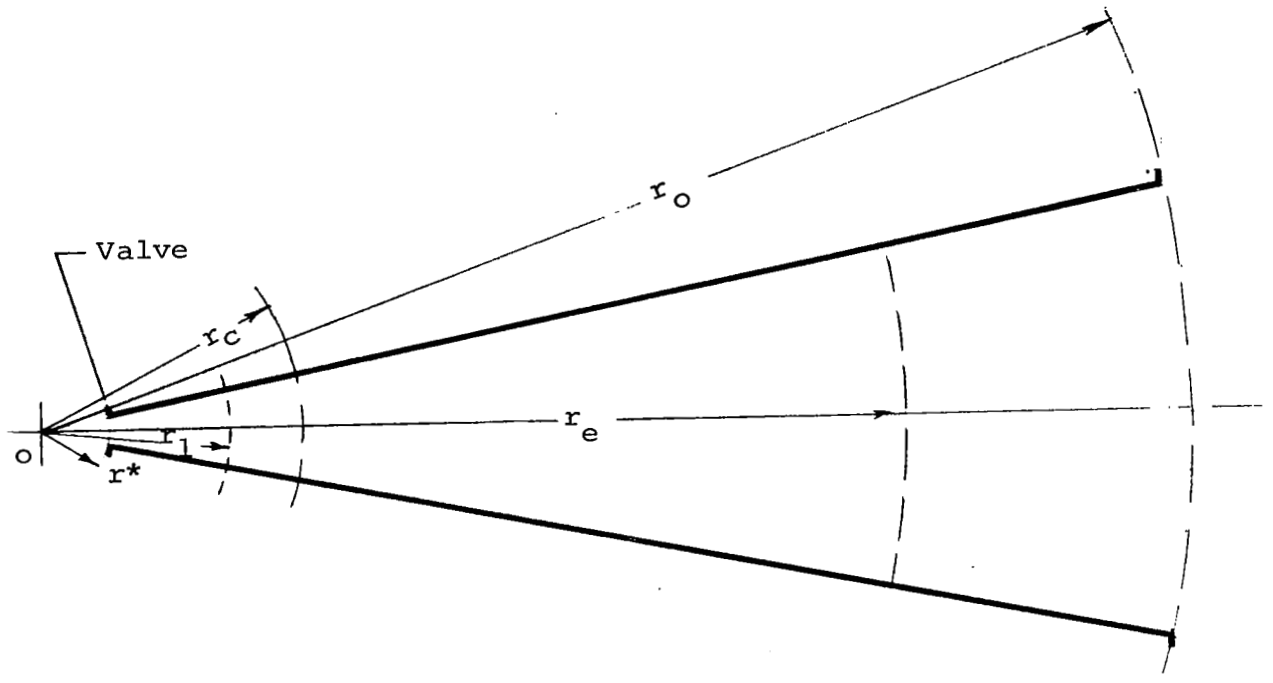

FIGURE 3 - CONICAL DUCT NOMENCLATURE

$$\frac{S}{S^*} = \left(\frac{2}{\gamma+1}\right)^{\frac{1}{\gamma-1}} \frac{1}{\sqrt{\frac{\gamma+1}{\gamma-1}\left[\left(\frac{\rho_1}{\rho_\infty}\right)^2 - \left(\frac{\rho_1}{\rho_\infty}\right)^{\gamma-1}\right]}} \tag{2}$$

$$w = \left(\frac{2}{\gamma+1}\right)^{\frac{1}{2}\frac{\gamma+1}{\gamma-1}} S^* a_\infty \rho_\infty \tag{3}$$

where S^* is given by Eq. (3) and at every instant of time w the mass flow is considered constant throughout the region $r^* < r < r_c$. In Eqs. (1) and (2) the subscript 1 is used to denote the density and velocity upstream of the shock interface. The local value of Mach number in this region is given by

$$M_1 = \sqrt{\frac{2}{\gamma-1}\left[\left(\frac{\rho_\infty}{\rho_1}\right)^{\gamma-1} - 1\right]} \tag{4}$$

and the condition $M_1 = 1$ determines the required mass flow rate as indicated by Eq. (3). Since the simulator facility is built with a relatively small divergence angle in the duct, a plain shock can be assumed to exist at $r = r_i$. Hence the classical shock wave equations can be used to determine the change in properties of the flow field gas across the shock. In particular, if M_{1i} denotes the Mach number immediately upstream of the shock interface the ratio of the stagnation pressure p_∞ upstream of the shock to the stagnation pressure p_o downstream of the shock is given by

$$\frac{p_\infty}{p_o} = \frac{\frac{\gamma+1}{2}}{\left[(\gamma+1)M_{1i}^2\right]^{\frac{2\gamma}{\gamma-1}}} \left[2 + (\gamma-1)M_{1i}^2\right]^{\frac{\gamma}{\gamma-1}} \left[2\gamma M_{1i}^2 - (\gamma-1)\right]^{\frac{1}{\gamma-1}} \tag{5}$$

Equation (5) is written with the assumption that the pressure p_o is the ambient pressure in the acoustic section of the cone, and is assumed to be constant during the period of time the wave propagates in the horn.

The set of Eqs. (1), (2), (4) and (5) are the basic operating equations needed to design the mass control valve used on the simulator facility. Specifically, by choosing the pressure p_∞ of

the reservoir, Eq. (5) will provide the value of the Mach number in the supersonic flow at the shock interface. Then, by means of Eq. (4) the density ratio ρ_∞/ρ_1 can be obtained. Then using Eq. (1) and (3) the value of the throat area S* as a function of w can be computed. Equation (2) with the value of S* then can be used to determine the position r_1 of the shock interface. It may be noted that as the mass flow increases, the shock interface moves downstream reaching a maximum distance when the mass flow rate attains its maximum value. Ultimately the motion of the shock interface controls the rise time capability of the device.

A sample calculation of the various parameters is briefly given below.

Assume a driving pressure of 10 atm., then via Eq. (3) the area S_c^* corresponding to position r_c is

$$S_c^* = \frac{w}{a_\infty \rho_\infty \left(\frac{2}{\gamma+1}\right)^{\frac{1}{2}} \frac{\gamma+1}{\gamma-1}}$$

for $a_o = 330$ m/sec, $\rho_\infty = 10\ \rho_o = 12.25$ kg/m^3

$$a_o \rho_\infty = 4050 \text{ kg/m}^2 \text{ sec}$$

$$\left(\frac{2}{\gamma+1}\right)^{\frac{1}{2}\frac{\gamma+1}{\gamma-1}} \cong \left(\frac{1}{1.2}\right)^3 = \frac{1}{1.728}$$

Hence $S_c^* = 1.728\ \frac{w}{4050} = 4.32 \times 10^{-4}\ w.$

From Eq. (17)

$$w_{max} = \frac{1}{4\gamma}\ \rho_o a\ \frac{a\tau_o}{r_e}\ \frac{\bar{p}_e}{p_o}\ S_o \quad (\rho = r_e^2 \Omega)$$

$$= 101\ \frac{a\tau_o}{\gamma r_o}\ \frac{\bar{p}}{p_o}\ S_o$$

where S_o is the area of the end opening.

Assume the conditions at the test section (S_o) to be,

$S_o = 5.76 m^2$ (8x8 ft)

$r_o = 30m$

$\tau_o = .1$ sec

$\frac{\bar{p}}{p} = 10^{-3}$ (~2 psf)

$w_{max} = .42$ kg/sec

Then, $S^* \simeq 2.6$ cm^2.

A number of possible design configurations were considered for the mass control valve. The basic requirements for such a valve are that it can pass a large mass flow at peak opening, that the transition from no flow to flow can be sharp and that the flow characteristics can be tailored easily so that the required mass flow profiles can be obtained. Although the slide valve mechanism used in the pilot facility produced the required mass flow profiles, the amount of mass that could be passed through such a valve is highly limited because of its one-dimensional character. In addition, except in the full open condition the orifice "appears" as a free jet and thus generates a significant amount of background noise. Other configurations that were considered were a moving belt and a cam valve as well as a flexible wall type orifice. However, the requirements for large mass flow and suitably shaped nozzle to reduce jet noise ultimately led to the design of a plug valve.

In Figure 4 the schematic of this valve is shown. Three basic types of operation are possible in this arrangement. First, the valve pintle or plug may be programmed to open and then close symmetrically with a constant velocity and hence the mass flow characteristics are determined by the profile on the plug. A second mode of operation allows that the velocity of the piston can be varied in a predetermined fashion and that a linear mass flow characteristic is always established on the plug. A third possibility exists which does not require reciprocating motion during the operation. A plug can be constructed with both an increasing and decreasing conical section such that with a single constant velocity stroke, the entire mass flow profile can be obtained. This latter configuration,while the easiest to obtain

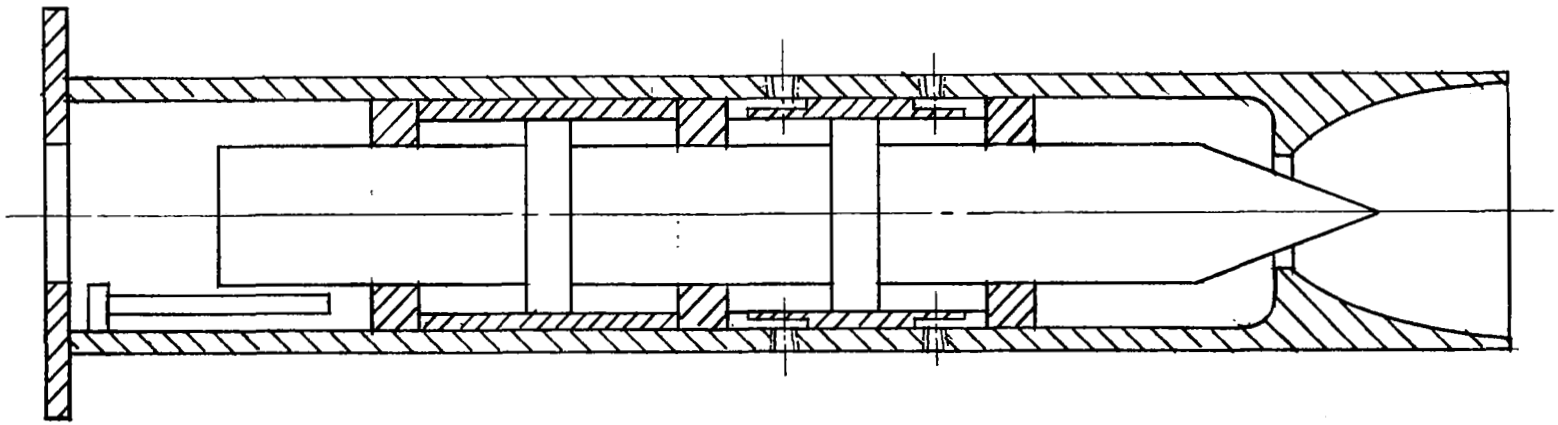

FIGURE 4

SCHEMATIC OF PLUG VALVE

from a dynamic point of view presents an obstruction downstream of the sonic orifice which may generate excessive noise or interfere with the flow.

For the initial operation of the device the first mode configuration was chosen. To obtain the nominal N-wave, a parabolic mass flow characteristic is needed. In the cylindrical geometry of the plug valve this consists of a linear tapered cone, assuming that the plug moves at constant velocity. The basic dimensions of the plug valve were developed by the conditions established in the analysis and are such that for the longest anticipated wavelength a suitable overpressure of 2 to 3 lbs. per square foot can be obtained. Under these conditions the mass flow is on the order of 50 lbs./sec at the maximum opening of the valve. With nominal pressure of 1000 psi in the plenum, a 2" orifice is required for this mass flow. (See Figure 5 for scale drawing.)

For any of the modes of operation outlined above, it is desirable that no unbalanced pressure loading exist on the plug so that the driving power requirement reduces to that needed only for the inertial component. Note that if no compensation for the varying load on the plug is made, with a 1000 psi pressure in the plenum, an unbalanced force on the plug amounting to 6000 lbs. can be developed. This load would vary from 0 to the maximum value as a function of the opening of the valve. This in turn would influence the constant velocity character required to obtain the desired profile. To reduce the effect of this varying load, a compensating element was introduced into the rear section of the plug valve. This compensation is obtained by taking a sample pressure from the edge of the tapered plug and transmitting this pressure to a compensating piston located behind the driving piston. In principle this system will reduce the variation in load by a factor of 10 over the entire range of stroke.

The driving force supplied to the plug shaft is obtained via a hydraulic system. The hydraulic system is composed of two 3 cubic foot tanks, each containing water with soluble oil which is used as the hydraulic fluid. Since the demand on the hydraulic system is basically of an impulse nature the tanks are alternately pressurized and the return from the hydraulic piston would be directed to the non-pressurized tank. The logic for this arrangement is obtained using large check valves and is shown schematically in Figure 6. The fundamental power capacity of this hydraulic system is limited only by the size of the hoses used to connect

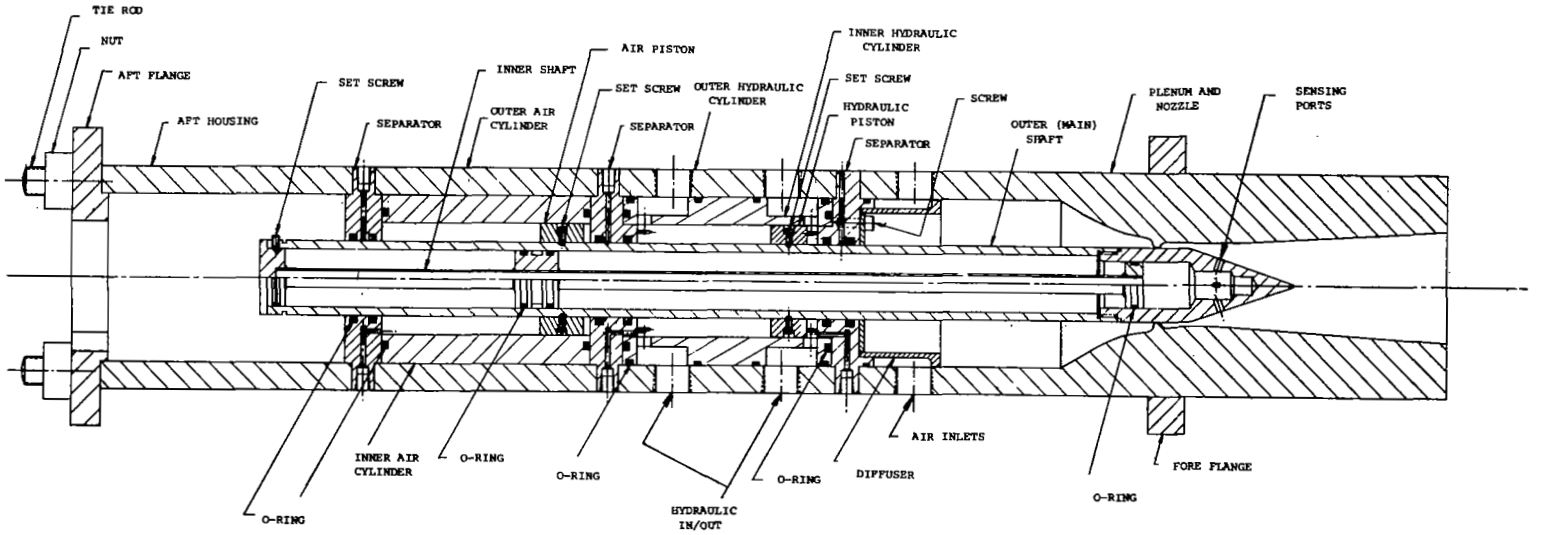

FIGURE 5: SCALED DRAWING OF PLUG VALVE (1/4" = 1")

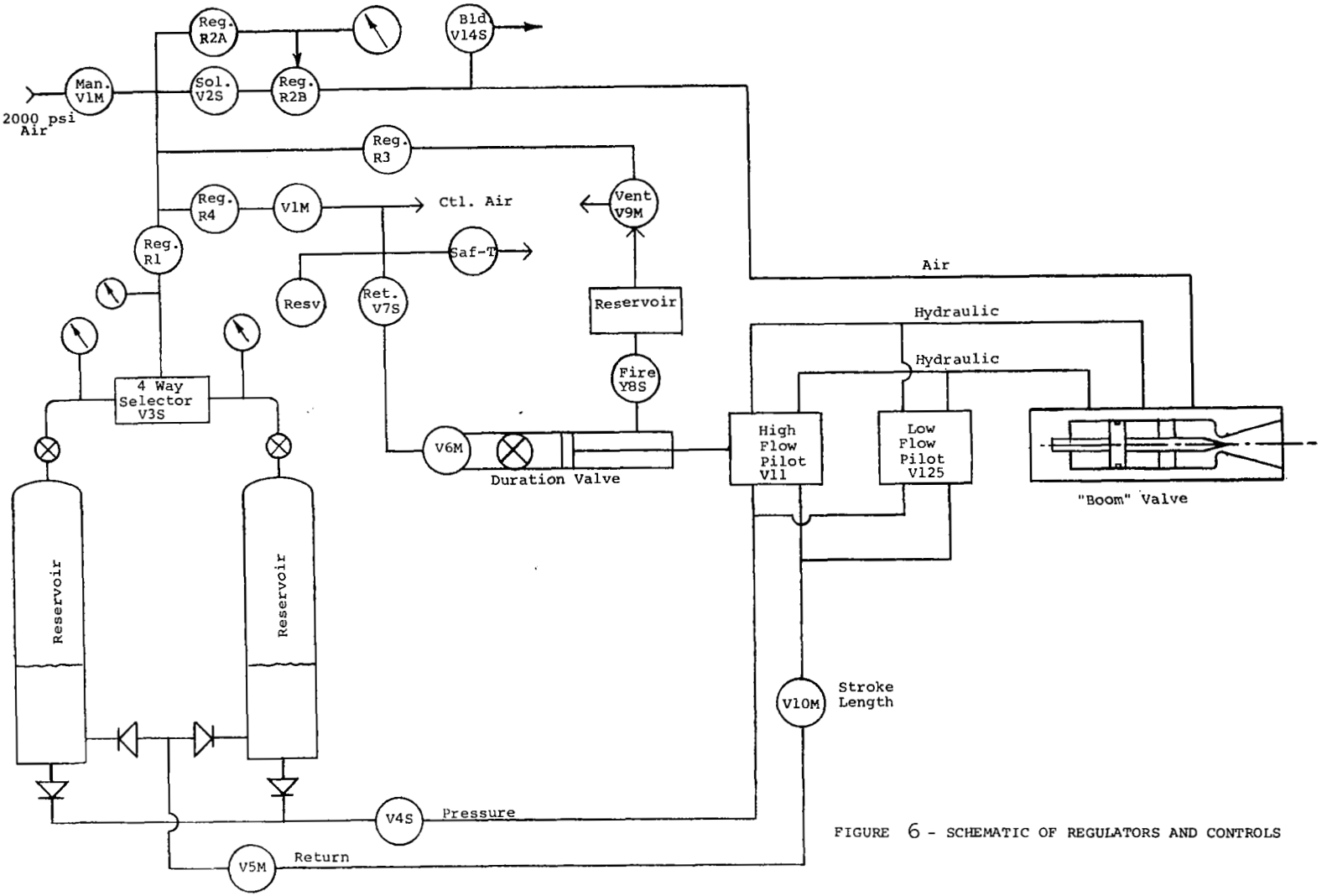

FIGURE 6 - SCHEMATIC OF REGULATORS AND CONTROLS

the valving. The initial configuration has capability of 50 gals. per minute at 3000 psi hydraulic pressure which roughly corresponds to 50 horsepower.

From the schematic in Figure 6 it can be seen that the pressure output of the hydraulic system can flow through either of two valves, v-11 or v-12, and into the plug valve driving piston. The choice of valve depends upon the type of operation; whether it be manual or high speed programmed. To obtain the constant velocity of the piston as required for the initial mode of operation, a restricting orifice is placed in the hydraulic line so that the major drop in pressure occurs across this orifice so that the flow rate is essentially constant and thus the piston displacement is linear with time. The basic mechanical operation of this valve was highly successful up to periods as short as 30 msec and as long as 1/2 sec.

The original air supply requirement was not sized to meet the demands of the long wavelength high pressure flow condition. During such operations of the valve, when the plug is significantly open, the plenum pressure which is intended to be constant shows a significant drop as indicated by the lower trace of Figure 7. The position of the plug is indicated by the upper trace of this figure. Note that the first inch of travel of the pintle was designed not to allow mass flow in this initial configuration so that non-linear effects associated with the acceleration of the plug would be eliminated. The resulting N-wave produced consequently has a non-ideal behavior due to the changing plenum pressure as the valve opening changes.

A second difficulty with the plug valve is the transition from no flow to flow which should be sharp to obtain a rapid rise time. Due to the finite thickness of the orifice plate, there is always an inherent uncertainty in the flow transition. To improve this situation the throat thickness can be reduced and an additional step can be made on the plug to provide a more rapid transition of the flow during the initial stroking. Some typical results are shown in Figure 8 for the conditions indicated.

Another feature of the mass flow control system is that of the jet noise produced at the orifice. For many types of tests, this interference is of no consequence. However, for some physo-acoustic testing, the perceived noise in the frequency range corresponding to the jet noise, is highly noticeable. It may be noted that the frequency spectrum of the jet noise compared with

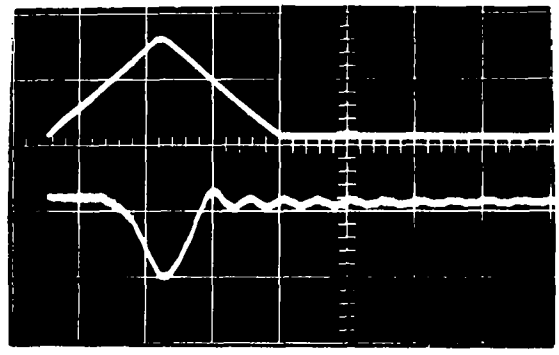

Time Scale:

1 division equals
0.1 seconds

Upper trace indicates position of valve pintle with each division corresponding to about 1 inch.

Lower trace is a measure of the plenum pressure with each division representing about 200 psi with the initial (and final) pressure about 400 psi.

FIGURE 7 - PLENUM PRESSURE RECORD

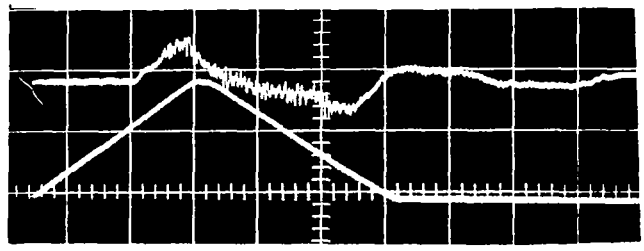

Time Scale:

1 division equals
0.1 seconds

a: Moderate rise time - long wave. About 3 psf overpressure. Note that the valve is full open about 75 ms before the center of wave because of the transit time down the duct.

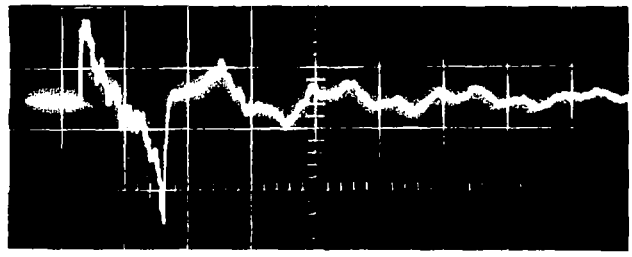

Time Scale:

1 division equals
0.1 seconds

b: Faster rise time. Peak overpressure about 10 psf.

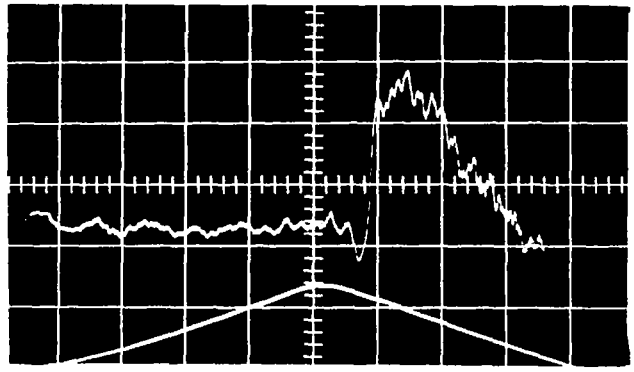

Time Scale:

1 division equals
20 millisec.

c: Expanded trace of a fast rise time wave. Signal above has been electrically filtered to reduce jet noise. Peak overpressure about 5 psf and rise time about 2 milliseconds.

FIGURE 8 - SOME TYPICAL INITIAL RESULTS

the frequency spectrum of the full scale sonic boom are significantly separated. Hence it is likely that acoustical filtering added in the duct can greatly reduce the jet noise problem. A crude attempt at providing such an acoustical filter was made and the results, while not perfect, showed promise.

Cone Termination

A significant portion of this research project was devoted to solving the problem of acoustic reflections from the open end of the conical duct. While the absorber is not required for very short wavelengths such as those used in scale model testing, it is clear that for long wavelengths (full scale booms) the reflected signal from the open end of the duct will interfere with the outgoing pressure wave generated by the source and combine to give a result which is not representative of the sonic boom signature. By performing a suitable analysis of the wave propagation in and at the end of the duct, a unique solution was obtained which permitted the realization of a small absorbing unit which would effectively cancel all of the wavelengths of practical interest. This analysis is presented below.

The calculations presented in Appendix A assume that no reflection occurs at the end of the cone which would make the function Φ_2 vanish in Eqs. (A4) and (A5). In practice, this condition cannot be achieved exactly and particular attention has been given to the problem of reducing the valve of Φ_2, at least in the range of frequencies of primary interest.

In general the physical termination at the end of the cone can be represented by an acoustical impedance Z_w. By Figure 1 it can be seen that at $r = r_o$ corresponding to the end of the conical duct Eqs. (A4) and (A5) lead to:

$$\left[\frac{aZ(\omega)}{\gamma p_o}\left(1 + \frac{a}{i\omega r_o}\right) - 1\right] \Phi_1 \; e^{-\frac{i\omega r_o}{a}} =$$

$$\left[\frac{aZ(\omega)}{\gamma p_o}\left(1 - \frac{a}{i\omega r_o}\right) + 1\right] \Phi_2 \; e^{-\frac{i\omega r_o}{a}} \qquad (6)$$

The specific condition that there be no reflected wave is represented when Φ_2 is set equal to zero. Then $Z(\omega)$ is given by the complex

$$\frac{1}{Z(\omega)} = \frac{a}{\gamma p_o}\left(1 + \frac{a}{i\omega r_o}\right) \tag{7}$$

From this equation it is clear that it is impossible to terminate the cone at this position with a simple absorbing material which would correspond to only a real value of $Z(\omega)$.

In agreement with Eq. (A6), Eq. (7) shows that the radial velocity at $r = r_o$ is composed of two terms, the first being proportional to the pressure and the second being proportional to the time integral of the pressure. This second term cannot be neglected in the low frequency range when $\frac{\omega r_o}{a}$ is less than or equal to 1, i.e., when the parameter is defined by ξ in Eq. (A12) for $r - r_o$ is of the same order or larger than unity.

The first term on the right hand side of Eq. 7 corresponds to a conventional sound dissipation mechanism while the second term represents the inertial behavior due to the motion of the mass of gas. These considerations suggest the possibility of canceling the reflected wave by means of a termination which would consist of a moving absorber as represented by a scheme of Figure 9. In this figure consider that the piston is porous and

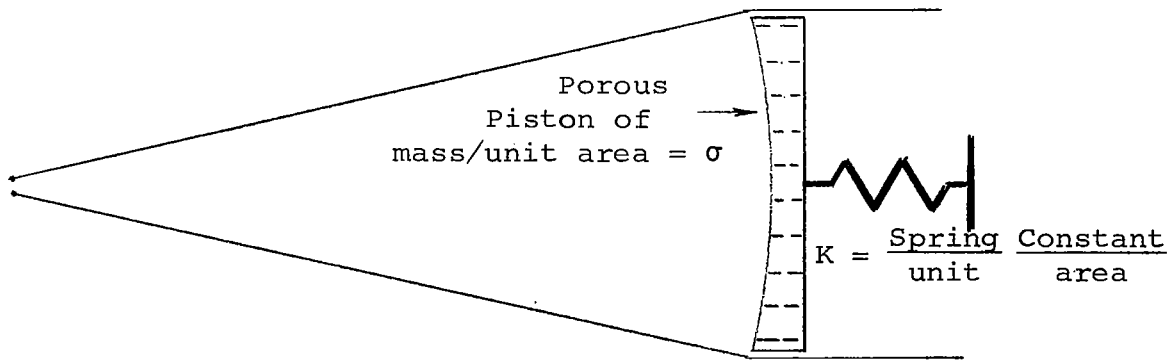

FIGURE 9. - SCHEMATIC OF MOVING ABSORBER CONCEPT

is free to move along the axis of the cone with wall friction R and an elastic restoring force shown by the spring K which is used to establish the equilibrium position. Assume that the driving force on the piston is due to the viscous effect of the air passing through the porous piston. Then the equation of motion of the piston can be written in the form of

$$p(r_o t) = R_1 \left[u_r(r_o t) - v\right] = \sigma \frac{\partial v}{\partial t} + Rv + K \int v \, dt \tag{8}$$

where v is the piston velocity, σ and K are the mass and spring constant per unit area respectively, R_1 is the resistance which corresponds to the viscous drag mechanism in the porous piston, also per unit area. The effect of mechanical friction is included as a factor R which is also given as equivalent resistance per unit area.

By means of Eq. (8) and the boundary conditions expressed by Eq. (6), the functions Φ_1 and Φ_2 of the outgoing and reflected waves are given by

$$\left[\frac{aR_1}{\gamma p_o}\left(1 + \frac{a}{i\omega r_o}\right) - 1 - \frac{R_1}{R + i\omega\sigma + \frac{K}{i\omega}}\right] \Phi_1 \, e^{-\frac{i\omega r_o}{a}} = \left[\frac{aR_1}{\gamma p_o}\left(1 - \frac{a}{i\omega r_o}\right) + 1 + \frac{R_1}{R + i\omega\sigma + \frac{K}{i\omega}}\right] \Phi_2 \, e^{\frac{i\omega r_o}{a}} \tag{9}$$

In an ideal situation where no mechanical friction effects exist (R = 0) and no elastic force is used to maintain the equilibrium position K = 0, then Eq. (9) will provide the values of viscous resistance and mass per unit area for the condition $\Phi_2 = 0$ if

$$R_1 = \frac{\gamma p_o}{a} = \rho_o a \qquad \sigma = \rho_o r_o \tag{10}$$

In practice the value of K can be chosen as small as required or eliminated if a manual repositioning is done after each operation of the simulator. And, by careful design, the mechanical resistance can be made small compared to the viscous resistance so that this quantity becomes only a perturbing effect. In order to evaluate the significance of real spring constant and real mechanical friction, the complete solution is given by Eq. (11)

$$\Phi_2(\omega) = \frac{ia(r_o \rho_o \omega^2 + i\omega R)\ \Phi_1 e^{-\frac{2i\omega r_o}{a}}}{2r_o^2 \rho_o \left[\omega^3 - \frac{iR\omega^2}{r_o p_o} - \left(\omega_o^2 - \frac{aR}{2r_o^2 \rho_o}\right)\omega + \frac{a\omega_o}{2ir_o}\right]} \tag{11}$$

where ω_o is the angular resonant frequency of the piston given by

$$\omega_o = \sqrt{\frac{K}{\sigma}} \tag{12}$$

If both K and R are sufficiently small, one obtains a reflected pressure signal $\bar{p}_r(t)$ at $r = r_o$ which is given in terms of the incident pressure $\bar{p}$ by

$$\bar{p}_r \sim \frac{a\omega_o^2}{2r_o} \iiint \bar{p}(\tau \cdot r_o)\ d^3\tau + \frac{a^2 R}{2r_o^2 R_1} \iint \bar{p}(\tau, r_o)\ d^2\tau \tag{13}$$

Thus, in the particular case of the N-wave prescribed by Eq. (A8), $\bar{p}_r$ attains its maximum value at $t = \tau_o$ which is given by

$$\frac{\bar{p}_r}{\bar{p}_e} \sim \frac{1}{24} \frac{a\tau_o}{r_o} (\omega_o \tau_o)^2 + \frac{1}{12} \left(\frac{a\tau_o}{r_o}\right)^2 \frac{R}{R_1} \tag{14}$$

which is valid as long as the ratio $R/R_1 \ll 1$. Within the fundamental error limitations of this absorber technique which occur at the very long wavelengths, as indicated by the integral expressions of Eq. (13), the moving piston concept as a useable end termination has the advantage of being a completely passive

arrangement. After a suitable matching or tuning has been achieved, almost complete cancellation of the reflected wave signal can be accomplished.

In order to reduce the theoretical requirements of this absorber into a practical device, an investigation was undertaken to determine the suitability of various materials to serve as the porous piston. Ideally, the material would exhibit a flow resistance which is constant over the range of flow velocities which will exist in the simulator, for instance, up to 200 centimeters per second. It was also deemed important in view of the uncertainty in the measuring techniques, to be able to vary the flow resistance by simply adding or removing layers of material. The value of the distributed mass, as required by Eq. (10) was conveniently large (500 lbs) so that the required rigid structure to hold the resistance material could be built.

However, the material which would produce the required flow resistance, as given by Eq. (10) was not so readily obtained or its signatures measured. Specifically, the flow resistance R_1 can be written in terms of the pressure drop divided by the velocity as given by

$$R_1 = \frac{\Delta p}{u} \tag{15}$$

where Δp equals the pressure differential across the absorber per cm^2 and u equals the velocity of the flow entering the absorber in cm per second. The value of R_1 from Eq. (10) for the

$1\ R_{ay} = \frac{1\ \text{dyne/cm}^2}{\text{cm/sec}}$ is approximately 40 R_{ay}/s.

A variety of materials were tested in a small (1"x2" test section) continuous flow open circuit wind tunnel. The tunnel was fabricated of lucite sheets and was equipped with sufficient pressure taps to provide the necessary data for material evaluation. The flow velocity was varied by altering the speed of the motor driven centrifical blower. Pressures were measured with inclined water manometers. Mass flow was determined by using a technique which consisted of measuring the time required to fill a specific volume.

Various fabrics made of both natural and synthetic fibers were tested as well as samples of 1/8" Hexcel honeycomb. In general, within the limits of accuracy obtainable with the

equipment, synthetic fibers provided the most nearly linear (with respect to velocity) flow resistance characteristics. Several representative curves are presented in Figures 10 and 11. In order to assess properly the relative linearity (or lack thereof) the significant data was normalized at the value corresponding to 60 cm/sec and results are shown in Figure 12.

The material selected as a result of these tests for initial use in the facility was 1/2 inch thick fiberglas blanket (0.75 lbs/ft^3 density). It may be noted from the data presented that for the velocity range of 60 to 150 cm/sec the flow resistance of this material is approximately proportional to the thickness, hence the resistance of the porous piston can be easily modified by changing the thickness of the fiberglas that was installed. This set of desirable characteristics of this material made it the initial candidate to be used in the absorber for this simulator facility. A schematic of the actual moving absorber is shown in Figure 13.

The results achieved by using this moving porous piston technique may be seen from Figure 14. The upper picture shows an incident pressure wave and the subsequent reflections obtained when the end of the conical duct is exhausting directly to the atmosphere. The lower picture illustrates the attenuation achieved with a similar input pressure wave after the absorber was installed at the exit of the facility. It is clear from this data that an order of magnitude reduction of reflected energy is obtained even by using this initial "untuned" design.

TECHNIQUES FOR USING THE FACILITY

The facility described has been demonstrated and does indeed simulate a sonic boom. It further incorporates features which make it a flexible device in varying the parameters of interest over a substantial range. This section will first describe this capability and then show how the facility should be used in conducting various sonic boom research studies.

Based on tests to date the following performance ranges should be available in the facility.

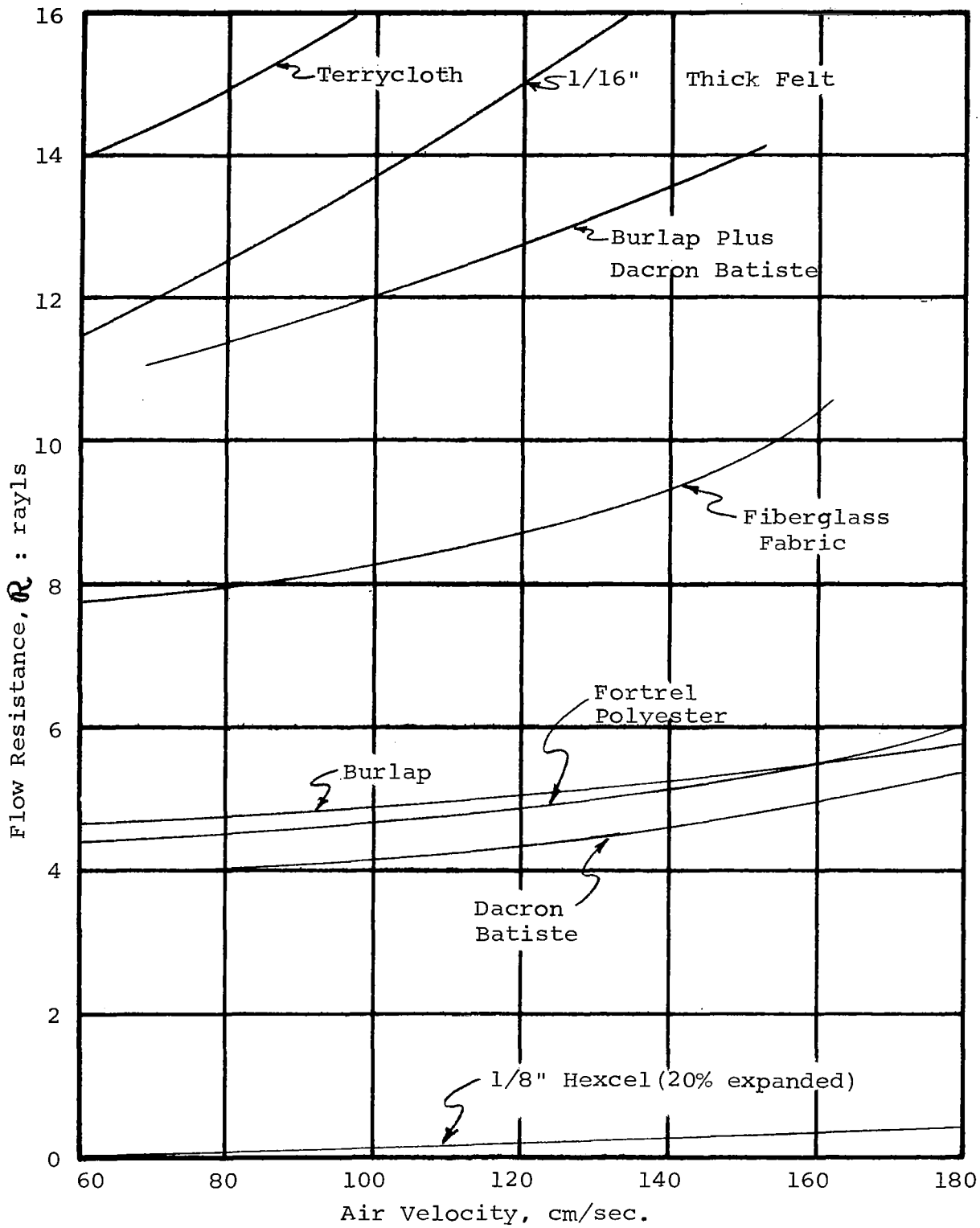

FIGURE 10 - FLOW RESISTANCE OF CANDIDATE ABSORBER MATERIALS

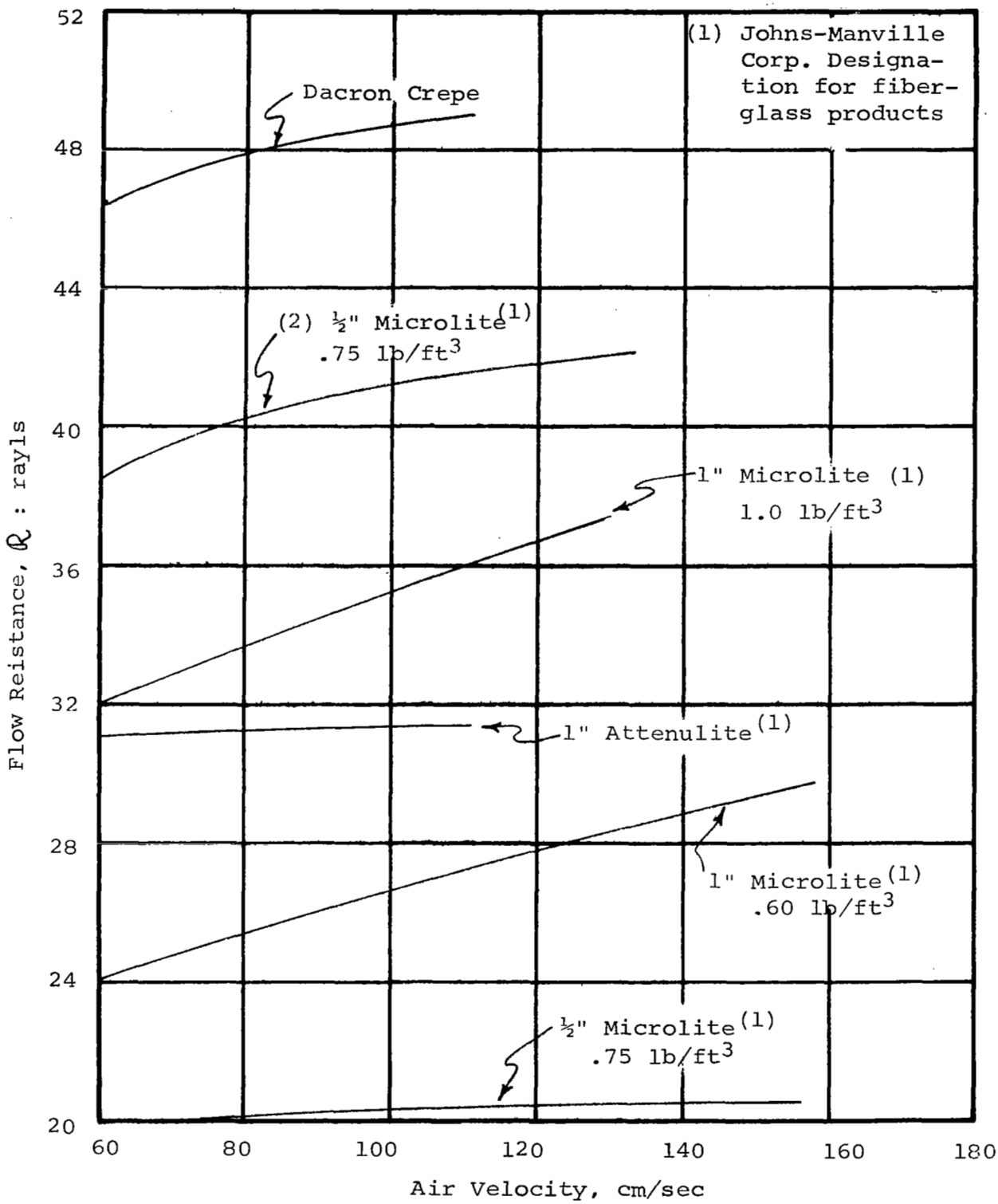

FIGURE 11 - FLOW RESISTANCE OF CANDIDATE ABSORBER MATERIALS

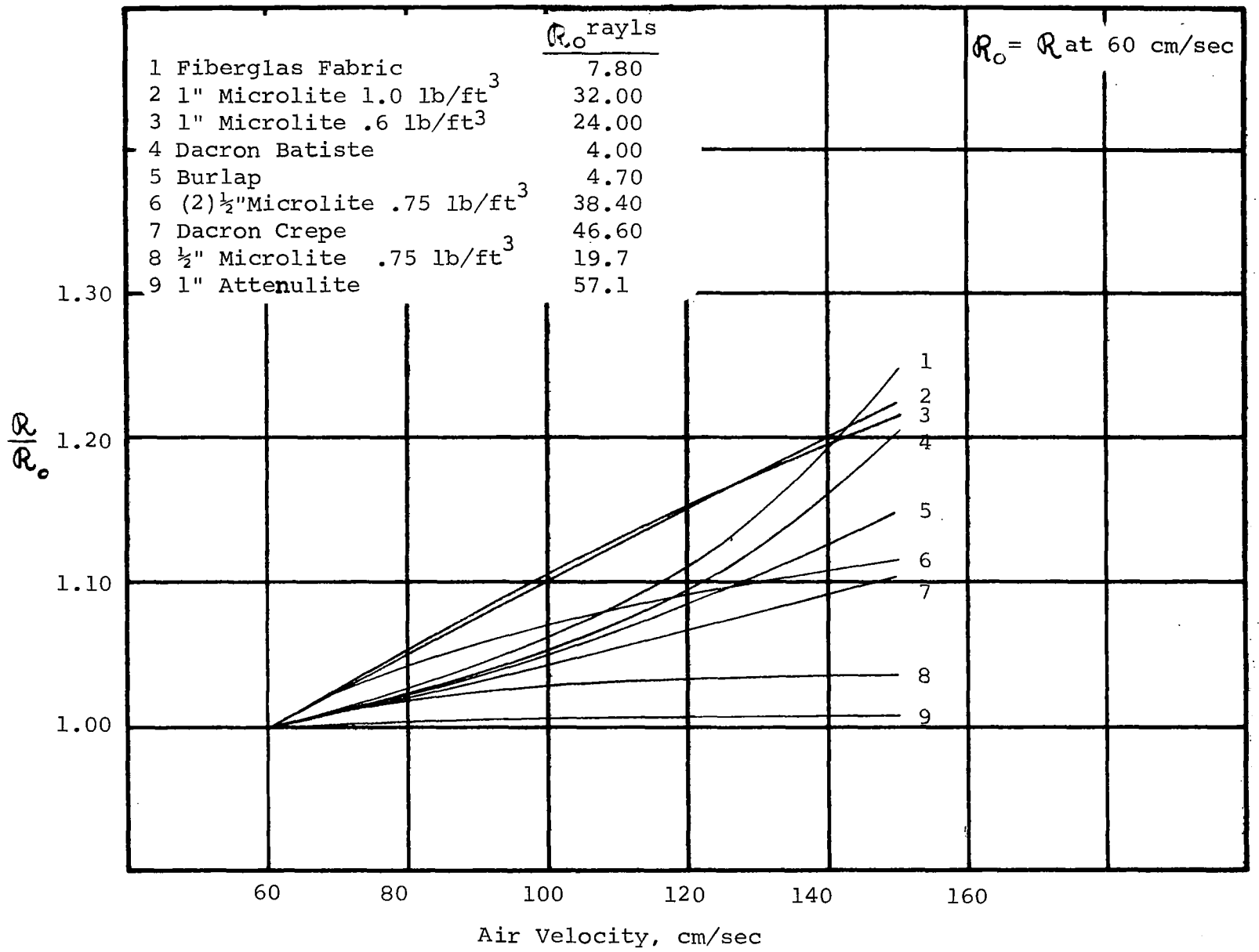

FIGURE 12 - NORMALIZED FLOW RESISTANCE OF CANDIDATE ABSORBER MATERIALS

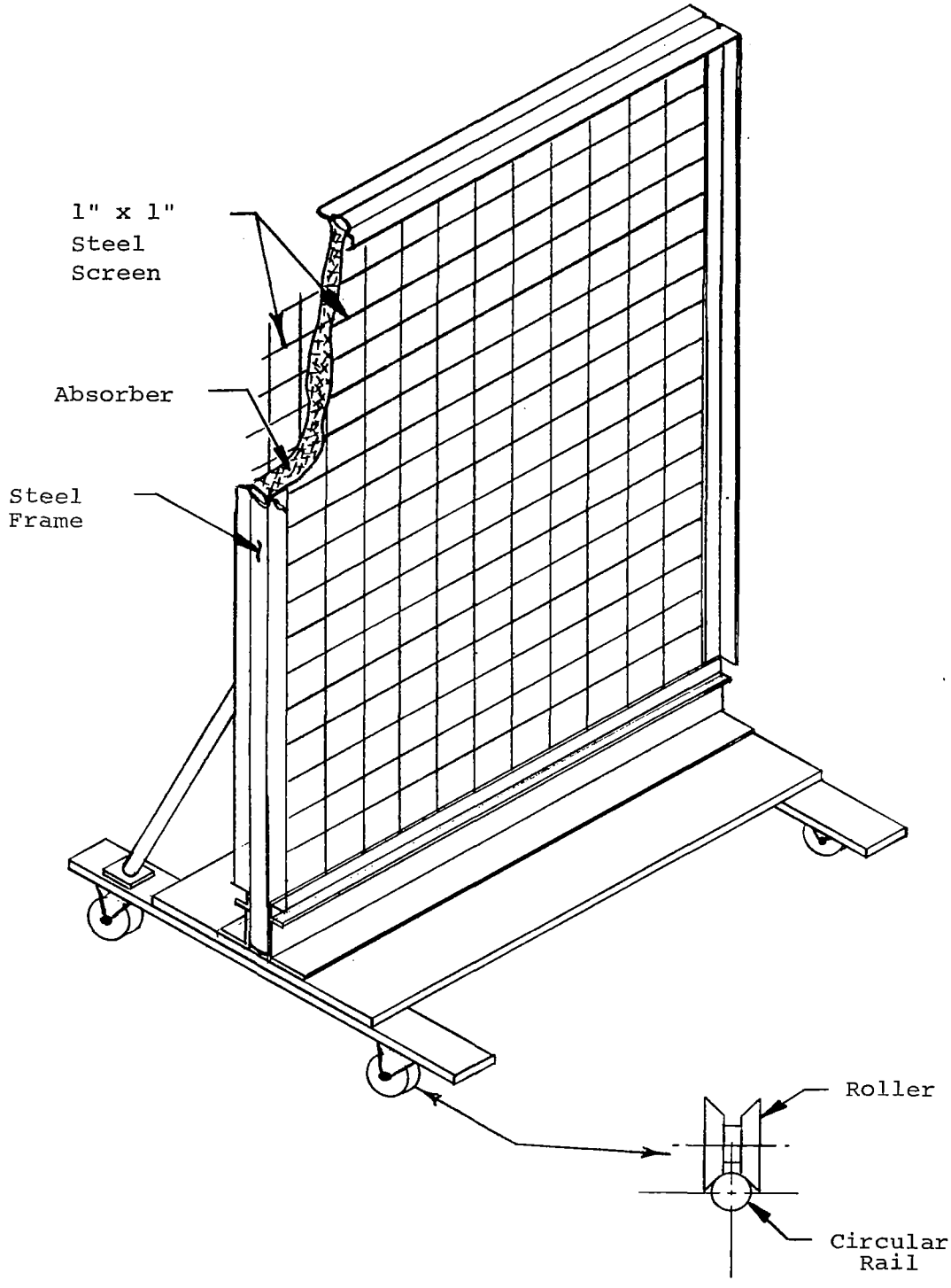
1" x 1"
Steel
Screen
Absorber
Steel
Frame
Roller
Circular
Rail

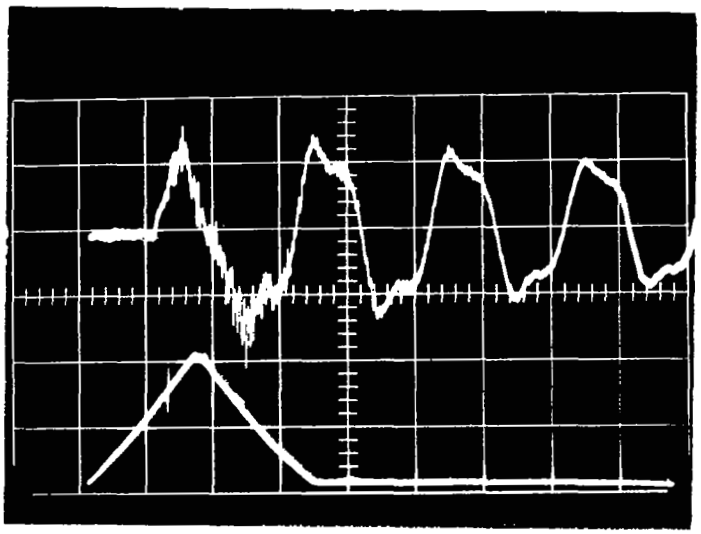

Without Absorber

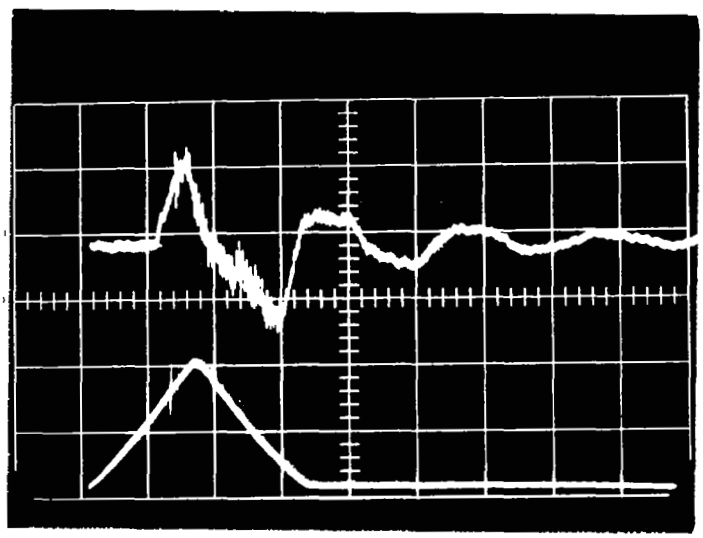

With Absorber

Each division equals 0.1 seconds. The moderate rise time is programmed by the mass flow control valve.

FIGURE 14 - DEMONSTRATION OF THE ABSORBER

Simulator Capability

Peak Pressure Level	up to 100 psf
Wavelength	1/4 ft - 500 ft
Period	300 μsec - 0.5 sec
Rise Time (minimum)	~ 1 millisecond
Repetition Rate (Typical)	up to 60/hr
Model Scale	1:1 to 1000:1
Maximum Test Station Area	8 feet square

It may be noted that the "typical" repetition rate is a function of the air compressor supply capability. Actually multiple booms separated by tenths of seconds can be produced if required. Not all the above have been actually demonstrated over their complete ranges, but no difficulty can be seen in doing so.

Many applications of the facility can be handled without any additions or modifications to the facility. For instance, Figure 15 shows a test set up for measuring the dynamic response of large structural models. In a similar manner the effects of terrain on sonic boom signatures can also be studied with scaled terrain models.

With a minimum modification the set up shown in Figure 16 can be used to test window response. Knockout sections exist in the side walls of the facility which will permit such a set up to be made.

Figure 17 shows a test set up for making psychoacoustic and other studies utilizing a full scale room built into a short extension of the present horn.

Atmospheric effects on sonic boom can be investigated by producing thermal gradients and thermal turbulence using heaters mounted in the floor of the horn. Turbulent airstreams can be produced by introducing jets normal to the two vertical walls of the horn.

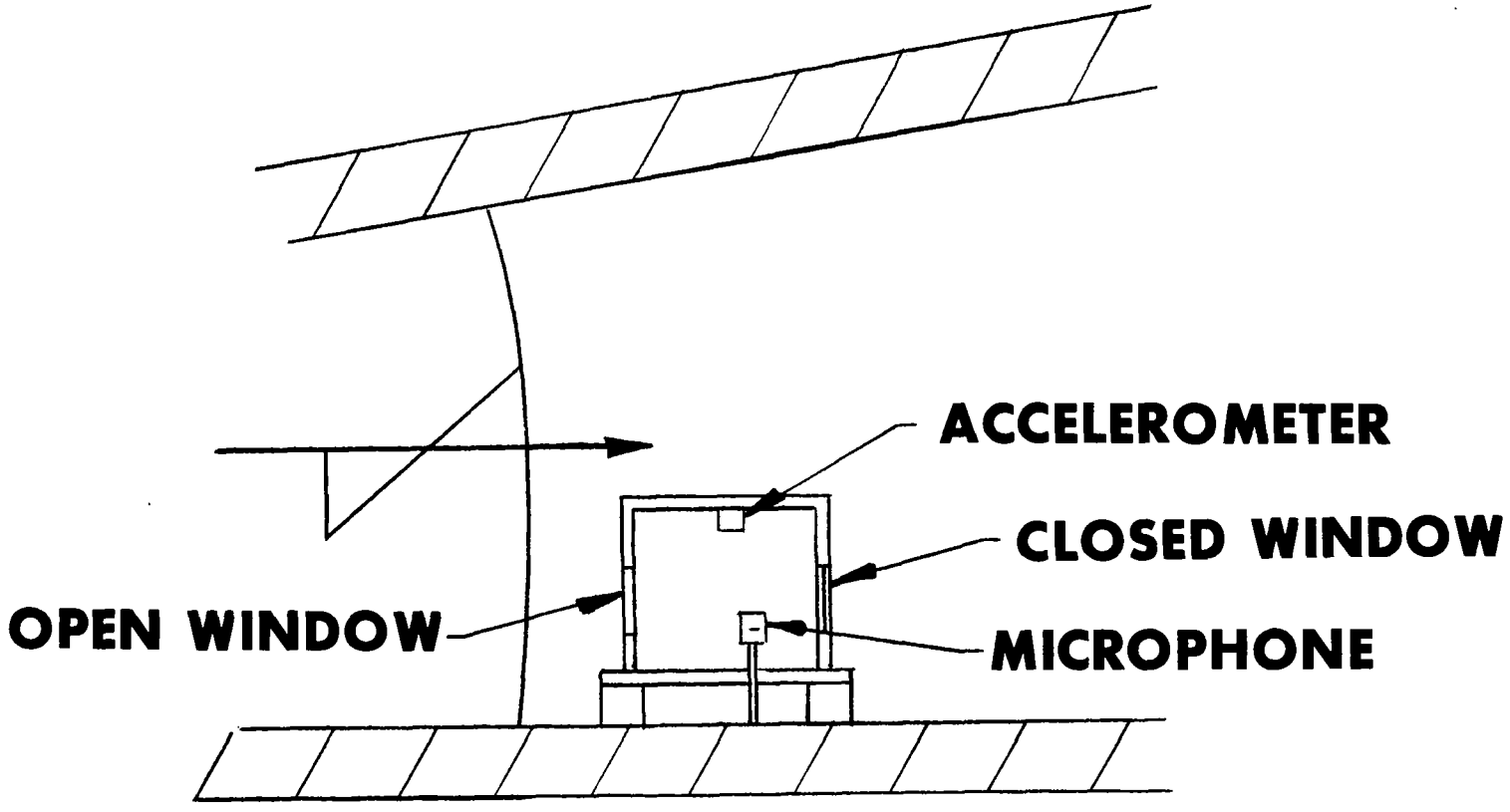

FIGURE 15

MEASUREMENT OF DYNAMIC RESPONSE OF LARGE STRUCTURAL MODELS

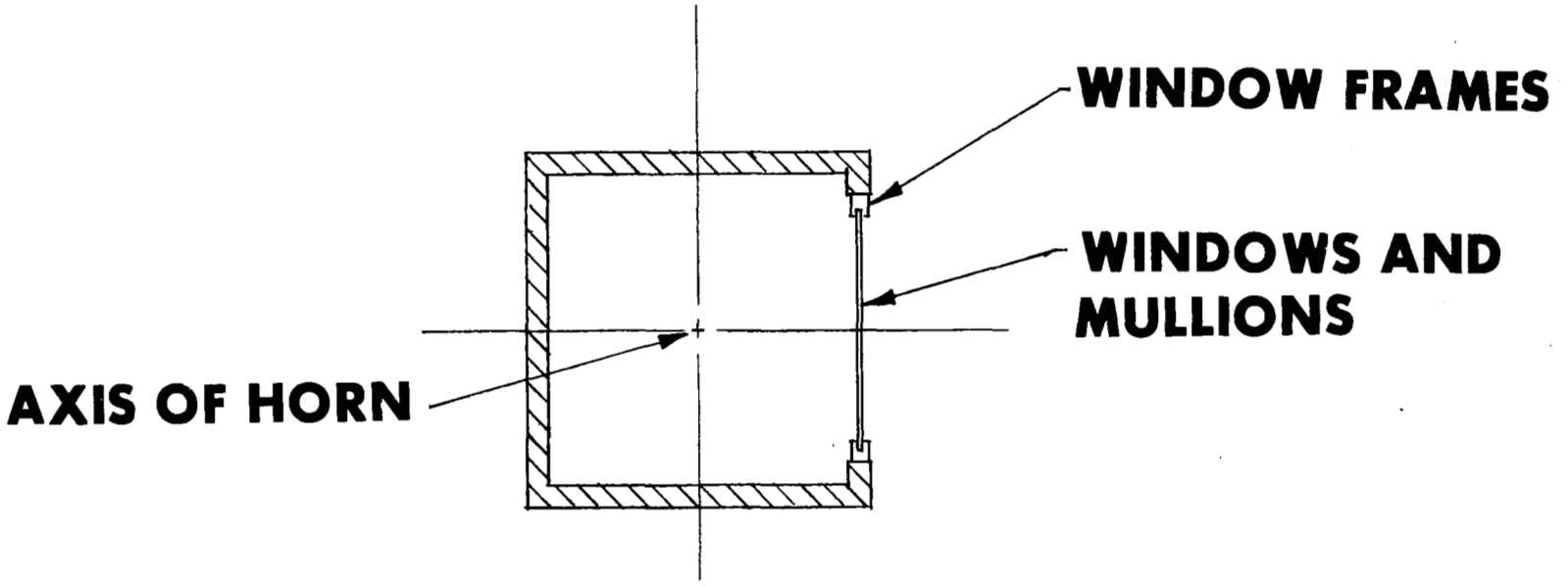

FIGURE 16

TEST OF GLASS WINDOW CONSTRUCTION AND MATERIALS

FIGURE 17

PSYCHOACOUSTIC STUDIES

The foregoing represent areas of current concern and indicate the approaches that could be used to employ this type of simulation for studies of these problems.

SUMMARY AND CONCLUSIONS

The primary purpose of this research program is to provide the fundamental relationships of the physical parameters important for this type of instrument, and to examine the potential solutions to the reflected wave problem. In support of this activity a facility was designed using the criteria established in the analysis. Pertinent drawings are included at the end of this section. The actual device, extending more than 100 feet, was constructed with an appropriate mass flow control valve and was equipped with all the required high pressure air and hydraulic systems essential for operation.

After the design concept of the moving piston type absorber was conceived and formulated, research was conducted to examine the materials and techniques required to reduce the concept to reality. The use of this passive end termination eliminated the requirements for a more sophisticated servo-operated mass control valve, which was initially contemplated.

An extensive program was devoted to obtaining the requisite materials for the moving absorber, after which a prototype design was constructed and tested. The initial results discussed in the section on Cone Termination indicate that the basic concept is, indeed, successful and the analysis of that section indicates the intrinsic small error for nominal wavelengths.

A series of more than 300 tests were performed to establish the behavior of the various systems. These tests included qualitative examination of test zones and the suitability of the wave generated for laboratory experiments.

The results thus far obtained are basically in agreement with the theory. However, some departures from the simple theoretical operation should be noted. It may be seen from the results presented, that in order to obtain the rapid rise time of Figure 8c,

an additional step was added to the mass flow profile. While this technique was successful, the details have not been fully explored. Second, as was pointed out in the section GASL-NASA SIMULATOR FACILITY, the plenum pressure in operation was not maintained constant for large openings of the plug valve. This was due, in part, to the actions of the various limiting orifices and the interactions of the upstream regulator system. The detailed requirements needed to maintain a constant plenum pressure for widely varying flow rates is of significance especially in considerations of larger scale facilities.

A third feature of the present simulator is that of the superimposed "jet" noise that is generated by the source. While it is clear that for many types of tests this noise is not important, the use of the simulator for psychoacoustic studies would require some reduction of this factor. It would appear promising that such a reduction can be obtained since the frequency spectra of the jet noise and the sonic boom are well separated, and in fact some preliminary steps that were taken indicate that substantial improvement is possible.

APPENDIX A

DERIVATION OF EQUATIONS GOVERNING

THE OPERATION OF THE GASL/NASA SIMULATOR

Assuming the conical duct as shown in Figure A1 with origin at 0, consider a spherical wave propagating in the positive direction with each variable a function of time and radial coordinate. In the region of the cone close to the origin, a large

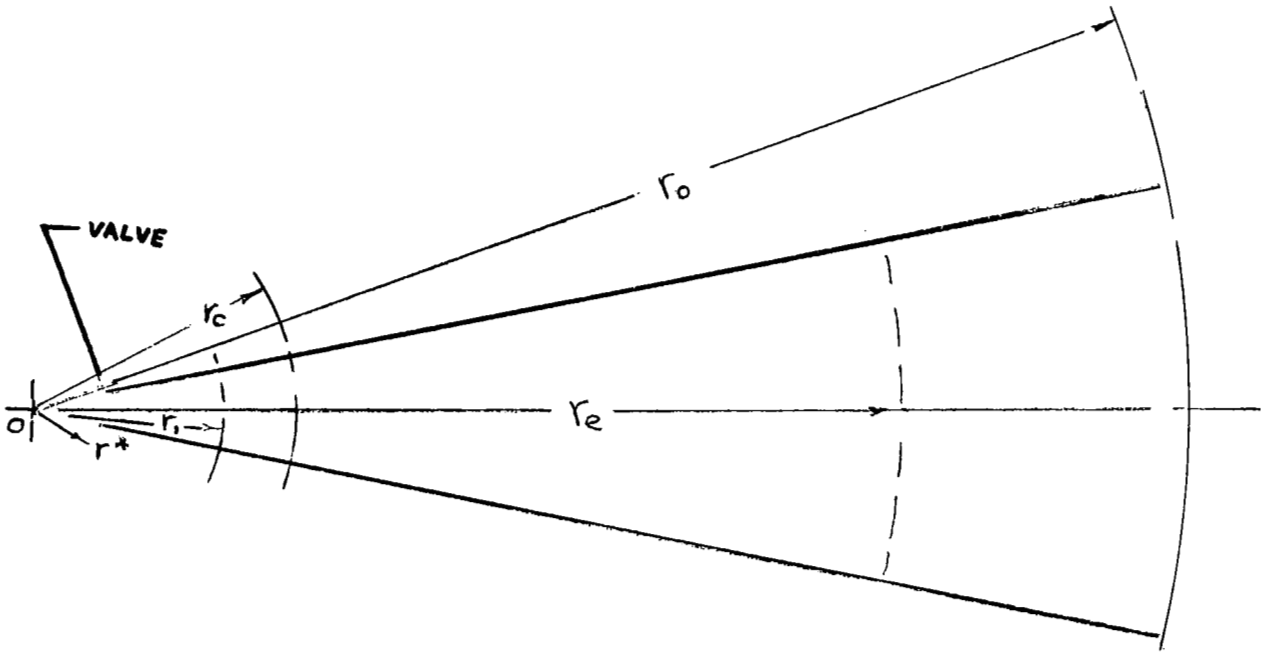

FIGURE A1 - CONICAL DUCT NOMENCLATURE

flow velocity and high pressure is generated to drive the pressure wave down the tube. In this small region the flow properties are essentially described by classical fluid dynamic

considerations. In the large portion of the cone, flow field velocities and pressure changes are small enough to allow the use of the acoustic approximation. Thus the governing equation for the pressure is

$$\nabla^2 \bar{p} - \frac{1}{a^2} \frac{\partial^2 \bar{p}}{\partial r^2} = 0 \tag{A1}$$

The flow field velocity, $\vec{u}$, is related to the pressure $\bar{p}$ by

$$\rho_o \frac{\partial \vec{u}}{\partial t} = - \nabla p \tag{A2}$$

For propagation with spherical symmetry, Eq. (A1) becomes

$$\frac{1}{r^2} \frac{\partial}{\partial r} \left(r^2 \frac{\partial \bar{p}}{\partial r}\right) - \frac{1}{a^2} \frac{\partial^2 \bar{p}}{\partial t^2} = 0 \tag{A3}$$

The general solution of Eq. (A3) may be written in the form

$$\bar{p} = \frac{1}{r} \int_{-\infty}^{+\infty} \left[\Phi_1(\omega) e^{-i\omega \frac{r}{a}} + \Phi_2(\omega) e^{i\omega \frac{r}{a}}\right] e^{i\omega t} \, d\omega \tag{A4}$$

where the first term represents a wave which propagates in the positive direction of the variable r, and the second term represents a wave propagating towards the origin of the cone. If the cone can be built so as to completely eliminate the reflection at the large end of the cone, the coefficient Φ_2 in Eq. (A4) is then equal to 0 and for this case only the first term is required to describe the wave pressure in the duct.

Assuming spherical symmetry, Eq. (A2) shows that the flow field velocity reduces to only the radial component, u_r. By combining Eqs. (A2) and (A4) the complete integral equation describing the radial velocity can be written

$$\frac{u_r}{a} = \frac{1}{\partial p_o r} \int_{-\infty}^{+\infty} \left[\left(i + \frac{a}{i\omega r}\right) \Phi_1 \, e^{-i\omega \frac{r}{a}} - \left(1 - \frac{a}{i\omega r}\right) \Phi_2 \, e^{i\omega \frac{r}{a}}\right] e^{i\omega t} \, d\omega \tag{A5}$$

The general Eq. (A5) can be solved once the acoustical properties of the large end of the cone are specified and the driving mechanism is prescribed which will permit evaluation of the boundary conditions and allow the computation of the two functions Φ_1 and Φ_2.

Consider the case that the reflection at the large end of the cone is eliminated and hence Φ_2 is equal to zero. Then by use of Eqs. (A4) and (A5) a new equation relating u_r to $\bar{p}$ may be written in the form of

$$\frac{\gamma u_r}{a} = \frac{\bar{p}}{p_o} + \frac{a}{r}\int_{-\infty}^{\tau} \frac{\bar{p}}{p_o}\, d\tau \tag{A6}$$

where

$$\tau = t - \frac{r}{a} \tag{A7}$$

Thus, assuming the reflection to be eliminated, Eq. (A6) allows the computation of mass flow which is required to obtain the prescribed pressure wave in any given section of the cone.

For example, assume a pressure wave at the position r_e of the cone to be an N-wave, which can be written in its idealized form as

$$\frac{\bar{p}}{p_o} = \begin{cases} 0 & \tau_e < 0 \\ \dfrac{\bar{p}_e}{p_o}\left(1-2\,\dfrac{\tau_e}{\tau_o}\right) & 0 < \tau_e < \tau_o \\ 0 & \tau_e > \tau_o \end{cases} \tag{A8}$$

where

$$\tau_r = t - \frac{r_e}{a} \tag{A9}$$

Here the constant $\bar{p}_e$ represents the initial pressure jump at $\tau_e = 0$, corresponding to the leading edge of the wave. Considering still that no reflection occurs from the large end of the cone, the pressure wave at any other position r is given by

$$\frac{\bar{p}}{p_o} = \frac{\bar{p}_e}{p_o} \frac{r_e}{r} \left(1 - \frac{2\tau}{\tau_o}\right)$$

$$\text{for } 0 < \tau < \tau_o \qquad \text{(A10)}$$

By virtue of Eq. (A6) and (A10) the flow field velocity, u_r is given by

$$\frac{\gamma u_r}{a} = \frac{\bar{p}_e}{p_o} \frac{r_e}{r} 1 - 2 \frac{\tau}{\tau_o} + \xi \frac{\tau}{\tau_o} \left(1 - \frac{\tau}{\tau_o}\right) \qquad \text{(A11)}$$

$$\xi = \frac{a\tau_o}{r} \qquad \text{(A12)}$$

From Eq. (A11) the function $\frac{\gamma u_r}{a}$ strongly depends upon the value ξ which is related to the distance from the origin as indicated by Eq. (A12), specifically at a large distance r such that $\xi << 1$ the term containing the ξ in Eq. (A11) is very small compared to unity, and thus

$$\frac{\gamma u_r}{a} \sim \frac{\bar{p}}{p_o} \qquad \text{(A13)}$$

Conversely at small distances of r such that $\xi >> 1$, the term containing ξ becomes dominant in Eq. (A11) except for values of τ close to both $\tau = 0$ and $\tau = \tau_o$. It is instructive to note that a distance where $\xi >> 1$ corresponds to the far field region in the propagation of an acoustic wave. On the other hand, $\xi \geq 1$ corresponds to the near field region where the flow behaves essentially as an incompressible gas with a velocity u_r which is inversely proportional to r^2. In the range of large values of

τ_o which may be of operational interest, the length of the facility is such that at $r = r_o$ the value of ξ is never small compared with unity.

To examine the mass flow requirements as controlled by the sonic orifice, the value of ξ will always be very large compared to unity, whence Eq. (A11) reduces to

$$\frac{\gamma u_r}{a} \simeq \frac{\bar{p}_e}{p_o} \frac{a r_e \tau}{r^2} \left(1 - \frac{\tau}{2\tau_o}\right) \tag{A14}$$

except for values of τ close to $\tau = 0$, $\tau = \tau_o$.

The function $\frac{\gamma u_r}{a}$ is related to the mass flow rate w through the use of

$$w = r^2 \Omega r_o u_r \tag{A15}$$

which yields for the ideal N wave.

$$w = r_e \rho_o \Omega \frac{a \bar{p}_e r}{\gamma p_o} \left[1 - 2\frac{\tau}{\tau_o} + \xi \frac{\tau}{\tau_o}\left(1 - \frac{\tau}{\tau_o}\right)\right] \tag{A16}$$

Again, close to the orifice where ξ is large,

$$w = \frac{r_e}{\gamma} \frac{\rho_o \bar{p}_e}{p_o} \Omega a^3 \tau \left(1 - \frac{\tau}{\tau_o}\right) 1 \tag{A16a}$$

and the maximum value of mass flow is found at $\tau = \frac{\tau_o}{2}$ and is given by

$$w_{max} = \frac{\bar{p}_e}{4\gamma p_o} r_e \Omega \rho_o a^2 \tau_o \tag{A17}$$

It can be seen that for the major portion of the prescribed N-wave according to Eq. (A14), the pressure is proportional to the true derivative of the mass flow which supports the basic concept considered in the pilot facility built at GASL.

Assume now that at $r = r_o$ the mass flow of air is obtained via a connection through a sonic area from a high pressure reservoir and thus the steady state mass flow through the valve is independent of the downstream condition which is given by

$$w = \left(\frac{2}{\gamma+1}\right)^{\frac{1}{2}\frac{\gamma+1}{\gamma-1}} S^* a_\infty \rho_\infty \qquad \text{(A18)}$$

where a_∞ and ρ_∞ are the speed of sound and the gas density in the reservoir, and S^* is the area of the sonic orifice.

If all the dimensions of interest in the sonic orifice are small compared to the wavelength corresponding to the maximum frequency of interest in the spectrum of the N-wave, then Eq. (A18) can be used to describe the new dependent flow rate due to a change in time of either the throat area S^* or a reservoir density, ρ_∞. Assume now that ρ_∞ is essentially constant during the time that the valve opens and closes to generate the N-wave. To obtain the complete description, the effect on the pressure wave due to mass flow rate function, Eq. (A16) is required to obtain the ideal pressure N-wave. The previous discussion suggests that we take the dominant term of Eq. (A16) to be the prescribed mass flow rate through the valve. Assume then that at a position $r = r_c$ close to the valve, the radial velocity is given by Eq. (A6) and thus the resulting pressure wave generated in the cone is given by

$$\frac{\bar{p}(\tau)}{p_o} = \frac{\gamma}{a}\,\frac{r_c}{r}\, e^{-\frac{a\tau}{r_c}} \int_{-\infty}^{\tau} e^{\frac{a\tau}{r_c}}\, \frac{\partial u_r}{\partial \tau}\, d\tau \qquad \text{(A19)}$$

and thus,

$$\frac{\bar{p}(\tau)}{p_o} = \frac{\bar{p}_e}{p_o}\,\frac{r_e}{r}\left[\left(1 + \frac{2r_c}{a\tau_o}\right)\left(1 - e^{-\frac{a\tau}{r_c}}\right) - \frac{2\tau}{\tau_o}\right] \qquad \text{(A20)}$$

for

$$0 < \tau < \tau_o \tag{A21}$$

Equation (A20) shows that for $\tau << \frac{r_c}{a}$ one has

$$\frac{\bar{p}(\tau)}{p_o} \sim \frac{\bar{p}_e}{p_o} \frac{r_e}{r} \frac{a\tau}{r_c} \tag{A22}$$

Thus at the beginning of the wave the pressure increases linearly with time and as previously discussed the quantity $\frac{r_c}{a\tau_o}$ may be small compared with unity. Therefore, after the partial transient described by Eq.(A22), Eq. (A20) reduces to

$$\frac{\bar{p}}{p_o} \sim \frac{\bar{p}_e}{p_o} \frac{r_e}{r} 1 - \frac{2\tau}{\tau_o} \tag{A23}$$

For values of τ larger than τ_o the pressure signal is given by

$$\frac{\bar{p}(\tau)}{p_o} = \frac{\bar{p}_e}{p_o} \frac{r_e}{r} \left[\left(1 + \frac{2r_c}{a\tau_o} \right) \left(1 - e^{-\frac{a\tau_o}{r_c}} \right) - 2 \right] e^{\frac{a}{r_c}(\tau - \tau_o)} \tag{A24}$$

and for $\frac{r_c}{a\tau_o} << 1$ then Eq. (A24) reduces to

$$\frac{\bar{p}(\tau)}{p_o} \sim - \frac{\bar{p}_e}{p_o} \frac{r_e}{r} e^{-\frac{a}{r_c}(\tau - \tau_o)} \tag{A25}$$

Figure A2 shows the solution of the function described by Eqs. (A20) and (A24). It can be observed that the smaller the value of $r_c/a\tau_o$ the closer the actual pressure wave will be to the ideal waveform described by Eq. (A8).